Proc. Natl. Acad. Sci. USA
Vol. 95, pp. 6037–6042, May 1998
Biochemistry

Stepwise *in vitro* affinity maturation of Vitaxin, an $\alpha_v\beta_3$-specific humanized mAb

(antibody engineering/angiogenesis/codon-based mutagenesis/phage expression/capture lift)

HERREN WU, GREGORY BEUERLEIN, YING NIE, HEIDI SMITH, BRUCE A. LEE*, MARY HENSLER, WILLIAM D. HUSE, AND JEFFRY D. WATKINS†

Ixsys, Inc., 3520 Dunhill Street, San Diego, CA 92121

Communicated by Leon E. Rosenberg, Princeton University, Princeton, NJ, March 27, 1998 (received for review January 12, 1998)

ABSTRACT **A protein engineering strategy based on efficient and focused mutagenesis implemented by codon-based mutagenesis was developed. Vitaxin, a humanized version of the antiangiogenic antibody LM609 directed against a conformational epitope of the $\alpha_v\beta_3$ integrin complex, was used as a model system. Specifically, focused mutagenesis was used in a stepwise fashion to rapidly improve the affinity of the antigen binding fragment by greater than 90-fold. In the complete absence of structural information about the Vitaxin-$\alpha_v\beta_3$ interaction, phage-expressed antibody libraries for all six Ig heavy and light chain complementarity-determining regions were expressed and screened by a quantitative assay to identify variants with improved binding to $\alpha_v\beta_3$. The Vitaxin variants in these libraries each contained a single mutation, and all 20 amino acids were introduced at each complementarity-determining region residue, resulting in the expression of 2,336 unique clones. Multiple clones displaying 2- to 13-fold improved affinity were identified. Subsequent expression and screening of a library of 256 combinatorial variants of the optimal mutations identified from the primary libraries resulted in the identification of multiple clones displaying greater than 50-fold enhanced affinity. These variants inhibited ligand binding to receptor more potently as demonstrated by inhibition of cell adhesion and ligand competition assays. Because of the limited mutagenesis and combinatorial approach, Vitaxin variants with enhanced affinity were identified rapidly and required the synthesis of only 2,592 unique variants. The use of such small focused libraries obviates the need for phage affinity selection approaches typically used, permitting the use of functional assays and the engineering of proteins expressed in mammalian cell culture.**

The growth of new blood vessels, termed angiogenesis or neovascularization, is tightly regulated and typically restricted to processes such as development, inflammation, and wound repair (reviewed in refs. 1 and 2). However, angiogenesis also occurs under certain abnormal circumstances such as cancer (3), rheumatoid arthritis (4), and eye diseases such as diabetic retinopathy and macular degeneration (5). In the case of cancer, the tumor cells often do not initially have a direct blood supply. However, a combination of growth factors, cytokines, and proteases secreted by tumor cells all promote angiogenesis, which, in turn, supplies nutrients to the tumor, permitting it to rapidly expand in size while also establishing a pathway for metastasis to distant sites (4).

Recently, a broader understanding of the mechanisms regulating angiogenesis has begun to emerge. For instance, integrin $\alpha_v\beta_3$, a member of a large family of cell surface proteins that mediate cell–matrix and cell–cell interactions, is up-regulated during angiogenesis (6). The murine mAb LM609 is specific for human $\alpha_v\beta_3$ integrin complex (7), blocks the interaction of $\alpha_v\beta_3$ with its ligands *in vitro* (8), and inhibits cell adhesion (7). Cytokines and growth factors stimulate angiogenesis and also have been postulated to influence vascular cell adhesion (9, 10), suggesting vascular cell adhesion plays a key role in angiogenesis *in vivo*. Consistent with this view, angiogenesis induced in a chicken chorioallantoic membrane model by basic fibroblast growth factor, tumor necrosis factor α, or human M21-L melanoma explants is inhibited by treatment with LM609 (6, 11). LM609 treatment, however, did not affect existing blood vessels, supporting previous observations that the $\alpha_v\beta_3$ receptor is up-regulated on neovasculature only. In addition to inhibiting angiogenesis, LM609 treatment induced apoptosis of vascular cells, leading to the regression of tumor explants (12). More recently, it has been demonstrated that LM609 inhibits the growth of tumors in a human skin transplant on a severe combined immunodeficient mouse (13). The tumors did not express the $\alpha_v\beta_3$ receptor, consistent with the inhibition of growth being mediated by the inhibition of angiogenesis.

Based on the inhibition of angiogenesis and the reduction of growth of carcinomas *in vivo*, inhibition of the $\alpha_v\beta_3$/ligand interaction has emerged as a strategy for the treatment of cancer. To date, the best-characterized, most-specific antagonist of the $\alpha_v\beta_3$ receptor is the LM609 murine mAb. However, the short serum half-life of murine mAbs caused by their immunogenicity in humans may limit the therapeutic potential of LM609 if an antiangiogenic approach to treating cancer requires chronic administrations.

One approach to circumventing this limitation is to humanize the murine antibody by grafting the murine complementarity-determining regions (CDRs) onto a human framework (14). Recently, the LM609 antibody was humanized by a previously described process (15) that uses phage expression technologies and codon-based mutagenesis. The humanized form of LM609, referred to as Vitaxin, retained the properties of the LM609 antibody as determined by *in vitro* and *in vivo* characterization and currently is in phase I human clinical trials for the treatment of solid tumors.

The goal of the present study was to improve the binding characteristics of Vitaxin to generate a more potent therapeutic agent. To do this, phage-expressed libraries of Vitaxin Fab variants were constructed. A limited initial mutagenesis strategy in which every position of all six CDRs was methodically and efficiently mutated was followed by the expression and screening of a combinatorial library consisting of the best mutations. This strategy resulted in the rapid *in vitro* affinity maturation of Vitaxin while requiring the synthesis of only 2,592 variants. The approach

The publication costs of this article were defrayed in part by page charge payment. This article must therefore be hereby marked "*advertisement*" in accordance with 18 U.S.C. §1734 solely to indicate this fact.

Abbreviation: CDR, complementarity-determining region.

*Present address: Biosite Diagnostics, Inc., 11030 Roselle Street, Suite D, San Diego, CA 92121.
†To whom reprint requests should be addressed. e-mail: jwatkins@cts.com.

is general, requiring no structural information, and appears to mimic the *in vivo* affinity maturation of Igs that occurs through iterations of somatic hypermutations followed by selection. The limited mutagenesis approach, resulting in smaller libraries, obviates the need for phage affinity selection techniques, and moreover, permits the use of functional assays that may not be adaptable to affinity enrichment schemes. Finally, characterization of the Vitaxin variants produced by this approach demonstrated a direct correlation between enhanced affinity for the $\alpha_v\beta_3$ receptor complex and the ability of the antibodies to inhibit both fibrinogen and vitronectin binding.

MATERIALS AND METHODS

Construction of CDR Libraries. Using the numbering system of Kabat *et al.* (16, 17), the residues chosen for mutagenesis of the CDRs (see Table 2) were: Gln^{24}–Tyr^{36} in light chain CDR1 (L1); Leu^{46}–Ser^{56} in light chain CDR2 (L2); Gln^{89}–Thr^{97} in light chain CDR3 (L3); Gly^{26}–Ser^{35} in heavy chain CDR1 (H1); Trp^{47}–Gly^{65} in heavy chain CDR2 (H2); and Ala^{93}–Tyr^{102} in heavy chain CDR3 (H3). Libraries were created for each CDR, with the oligonucleotides designed to mutate a single CDR residue in each clone. Because of the extended length of H2, two libraries mutating residues 47–55 (H2a) and 56–65 (H2b), respectively, were constructed to cover this region. Oligonucleotides encoding a single mutation were synthesized by introducing NN(G/T) at each CDR position as described (18). The antibody libraries were constructed in M13IXL604 vector (19) by hybridization mutagenesis as described (15, 20), with modifications. Briefly, the oligonucleotides were annealed at a 20:1 molar ratio to uridinylated Vitaxin template (from which the corresponding CDR had been deleted) by denaturing at 85°C for 5 min, ramping to 55°C over 1 h, holding at 55°C for 5 min, then chilling on ice. The reaction was electroporated into DH10B and titered onto a lawn of XL-1 blue.

Construction of Combinatorial Libraries. Degenerate oligonucleotides encoding both the wild-type and beneficial heavy chain mutations (H2, Leu^{60}→Pro; H3 Tyr^{97}→His; H3, Ala^{101}→Tyr; H3, Tyr^{102}→Ser, Thr, Asp, Glu, Met, Gly, Ala) were synthesized. Using hybridization mutagenesis at two sites simultaneously, as described above, the oligonucleotides were annealed at a 40:1 molar ratio to uridinylated template prepared from Vitaxin and three light chain mutations (L1, His^{32}→Phe; L3, Gly^{92}→Asn; L3, His^{96}→Leu). As a result, 256 variants were synthesized in four combinatorial library subsets.

Purification and Biotinylation of $\alpha_v\beta_3$. The $\alpha_v\beta_3$ receptor was purified from human placenta by affinity chromatography, as described (21), dialyzed into 50 mM Hepes, pH 7.4/150 mM NaCl/1.0 mM $CaCl_2$, containing 0.1% Nonidet P-40 (binding buffer) and incubated with 100-fold molar excess sulfosuccinimidobiotin for 3 h at 4°C. The reaction was terminated by the addition of 50 mM ethanolamine.

Screening of Phage Expression Libraries. Vitaxin variants were screened initially by a modified plaque lift approach, termed capture lift (22), in which the nitrocellulose was precoated with goat anti-human kappa antibody and blocked with BSA before application to the phage-infected bacterial lawn. After the capture of phage-expressed Vitaxin variant Fabs, filters were incubated with 1.0 μg/ml biotinylated $\alpha_v\beta_3$ for 3 h at 4°C, washed four times, incubated with 2.3 μg/ml NeutrAvidin-alkaline phosphatase (Pierce) for 15 min at 25°C, and washed four times. All dilutions and washes were in binding buffer. Variants that bound $\alpha_v\beta_3$ were identified by incubating the filters for 10–15 min in 0.1 M Tris, pH 9.5 containing 0.4 mM 2,2′-di-*p*-nitrophenyl-5,5′-diphenyl-3,3′-[3,3′-dimethoxy-4,4′-diphenylene]ditetrazolium chloride and 0.38 mM 5-bromo-4-chloro-3-indoxyl phosphate mono-(*p*-toluidinium) salt (JBL, Northridge, CA).

Vitaxin combinatorial libraries were screened by ELISA (23). Briefly, a microtiter plate was coated with 10 μg/ml of a mAb, which recognizes a peptide tag (24) on the carboxy-terminus of the Vitaxin variant heavy chains. After capture of Fab from *Escherichia coli* lysates, the plate was incubated with 0.5–1 μg/ml biotinylated $\alpha_v\beta_3$ for 1 h at 25°C. The plate was washed seven times, incubated with 0.5 units/ml of streptavidin-alkaline phosphatase (1,000 units/ml; Boehringer Mannheim) for 15 min at 25°C, washed seven times, and developed as described (23). All dilutions and washes were in binding buffer.

DNA Sequencing. Single-stranded DNA was isolated and the heavy and light chain V region genes were sequenced by the fluorescent dideoxynucleotide termination method (Perkin–Elmer).

Expression and Purification of Soluble Fab. Fab was expressed as described (23) and was released from the periplasmic space by sonic oscillation. Briefly, cells collected from 1-liter cultures were lysed in 10 ml of 50 mM Tris, pH 8.0 containing 0.05% Tween 20. Fab was bound to a 1-ml protein A column (Pharmacia), which had been equilibrated with 50 mM glycine, pH 8 containing 250 mM NaCl, washed with the same buffer, and eluted with 10 ml of 100 mM glycine, pH 3 into one-tenth volume 1 M Tris, pH 8. Purified Fab was quantitated as described (23).

Characterization Assays. For ELISA titration of Fab on immobilized $\alpha_v\beta_3$, $\alpha_v\beta_5$, and $\alpha_{IIb}\beta_3$, Immulon II microtiter plates were coated with 1 μg/ml of purified receptor in 20 mM Tris, pH 7.4/150 mM NaCl/2 mM $CaCl_2$/1 mM $MgCl_2$/1 mM $MnCl_2$, washed once, and blocked in 3% BSA in 50 mM Tris, pH 7.4/100 mM NaCl/2 mM $CaCl_2$/1 mM $MgCl_2$ for 1 h at 25°C. Human $\alpha_{IIb}\beta_3$, purified from platelets, was obtained from Enzyme Research Laboratories (South Bend, IN), and $\alpha_v\beta_5$ was purified from placental extract depleted of $\alpha_v\beta_3$, as described (25). Just before use, the plates were washed two times and then were incubated 1 h at 25°C with various dilutions of Fab. The plates were washed five times, incubated 1 h at 25°C with goat anti-human kappa-alkaline phosphatase diluted 2,000-fold, washed five times, and developed as described (23). All dilutions and washes were in 50 mM Tris-HCl, pH 7.4/100 mM NaCl/2 mM $CaCl_2$/1 mM $MgCl_2$.

Vitaxin variants were tested for inhibition of ligand binding as described (8) except the binding of biotinylated human fibrinogen (Calbiochem) was detected with 0.5 μg/ml of NeutrAvidin-alkaline phosphatase.

Inhibition of the adhesion of 4×10^4 M21 cells to fibrinogen by the Vitaxin variants was performed as described (26).

BIAcore Analysis. The kinetic constants for the interaction between $\alpha_v\beta_3$ and Vitaxin variants were determined by surface plasmon resonance measurements using a BIAcore 2000 instrument (Biacore, Uppsala, Sweden). Purified $\alpha_v\beta_3$ receptor was immobilized to a (1-ethyl-3-[3-dimethylaminopropyl]carbodiimide hydrochloride)/*N*-hydroxysuccinimide-activated sensor chip by injecting 30 μl of 15 μg/ml $\alpha_v\beta_3$ in 10 mM sodium acetate (pH 4). To obtain association rate constants (k_{on}), the binding rate at five different Fab concentrations ranging from 5 to 40 μg/ml in 50 mM Tris·HCl, pH 7.4/100 mM NaCl/2 mM $CaCl_2$/1 mM $MgCl_2$ was determined at a flow rate of 10 μl/min. Dissociation rate constants (k_{off}) were the average of five measurements obtained by analyzing the dissociation phase at an increased flow rate (40 μl/min). K_d was calculated from $K_d = k_{off}/k_{on.}$ Sensorgrams were analyzed with the BIAevaluation 2.1 program. Residual Fab was removed after each measurement with 10 mM HCl, 2 mM $CaCl_2$, and 1 mM $MgCl_2$.

RESULTS

Library Design. To optimize the affinity of Vitaxin *in vitro*, an M13 phage system that permits the efficient synthesis, expression, and screening of libraries of functional antibody fragments (Fabs) was used. Because of the absence of precise structural information about the interaction between Vitaxin and the $\alpha_v\beta_3$ receptor, the contribution of each of the six CDRs of the Ig heavy and light chains was assessed. The CDRs were defined broadly based on a combination of sequence variability (16) and antibody structural models (27, 28). Thus, one library was constructed for each CDR, with the exception of H2,

which was split into two libraries because of its long (20 amino acids) length. The libraries consisted of pools of variants, each clone containing a single amino acid alteration in one of the CDR positions. Using a previously described approach termed codon-based mutagenesis (18), every position in all of the CDRs was mutated, one at a time, resulting in the subsequent expression of all 20 amino acids at each CDR residue. The CDR libraries ranged in size from 288 (L3) to 416 (L1) unique members and contained a total of 2,336 variants.

Primary Screening. To permit the efficient screening of the initial libraries a highly sensitive plaque lift assay, termed capture lift (22), was used. Phage-expressed Vitaxin variants were selectively captured on nitrocellulose filters coated with goat anti-human kappa chain antibody, probed with biotinylated $\alpha_v\beta_3$, and detected with NeutrAvidin-alkaline phosphatase. Initially, biotinylated $\alpha_v\beta_3$ was titrated on lifts containing phage expressing only the Vitaxin parent molecule. Subsequently, the concentration of biotinylated $\alpha_v\beta_3$ was decreased to yield a barely perceptible signal. In this way, only clones expressing higher affinity variants were readily identified during screening of the variant libraries. After an exhaustive capture lift screening of ≥2,500 clones from each library 300 higher affinity variants were identified (Table 1). The greatest number of clones displaying improved affinity were identified in the H3 (185) and L3 (52) CDRs, though variants with improved affinity were identified in every CDR. Antibody variants identified by capture lift were characterized for binding to immobilized $\alpha_v\beta_3$ in an ELISA format (Fig. 1). Comparison of the inflection points of the binding profiles obtained from titrating variants on immobilized $\alpha_v\beta_3$ demonstrated that multiple clones displayed >3-fold improved affinity, confirming the effectiveness of using the capture lift in a semi-quantitative fashion (Fig. 1, compare squares and open triangles with closed circles).

DNA was isolated from clones displaying >3-fold enhanced binding and sequenced to identify the mutations that resulted in higher affinity. Based on sequence analysis of 103 variants, 23 unique mutations clustered at 14 sites were identified (Table 2). The majority of the sites of beneficial mutations were found in the heavy chain CDRs, with four located in H3, and three each in H2 (2a and 2b combined) and H1. Seven distinct and beneficial amino acid substitutions were identified at a single site within H3, tyrosine residue 102. The diverse nature of the substitutions at this site suggests that tyrosine residue 102 may sterically hinder Vitaxin binding to $\alpha_v\beta_3$. In support of this hypothesis, variants expressing the other aromatic amino acids (phenylalanine, histidine, and tryptophan) instead of tyrosine at residue 102 were never isolated after screening for enhanced binding.

Table 1. Capture lift screening of Vitaxin CDR libraries

Library	Size*	Screened†	Positives‡	Enhanced affinity§
H1	320	2,500	16	8
H2a	320	5,000	26	7
H2b	320	5,000	2	1
H3	320	2,500	98	78
L1	416	2,500	12	1
L2	352	3,250	7	1
L3	288	5,000	52	41

*Number of unique clones based on DNA sequence. Thirty-two codons are used to encode all 20 amino acids at each position.
†Phage-expressed libraries were plated on XL-1 blue/agar lawns at 500-1,000 plaques per 100-mm dish.
‡Positives are defined as clones that were identified in the initial screen, replated, and verified in a second capture lift assay.
§Soluble Fab was titrated against immobilized $\alpha_v\beta_3$ in an ELISA format. Based on comparison of the inflection point of the titration profiles, clones that displayed ≈3-fold enhanced affinity were selected for further characterization.

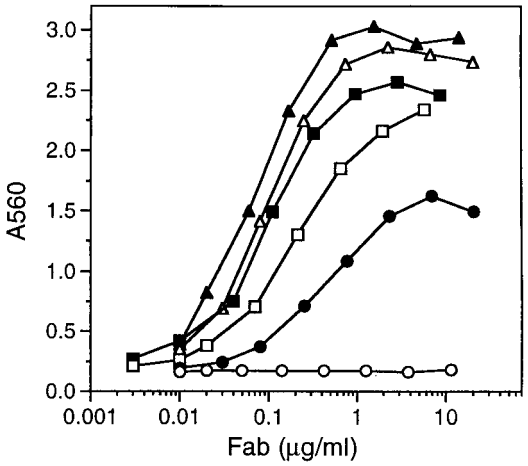

FIG. 1. Titration of variants and Vitaxin Fab on immobilized $\alpha_v\beta_3$. Bacterial cell lysates containing Vitaxin (●), variants with improved affinity isolated from the primary libraries (S102, ■; Y100, □; and Y101, △) or from the combinatorial libraries (clone 17, ▲), or an irrelevant Fab (○) were titrated on immobilized $\alpha_v\beta_3$ as described in *Materials and Methods*.

The affinities of select variants were further characterized by surface plasmon resonance measurements to determine the association and dissociation rates of purified Fab with immobilized $\alpha_v\beta_3$. Consistent with both the capture lift and the ELISA, the variants all displayed a lower K_d than the Vitaxin parent molecule (Table 2). Analysis of association and dissociation rates revealed that the majority of improved variants had slower dissociation rates while having similar association rates. For example, Vitaxin had an association rate of $18.0 \times 10^4\ M^{-1}\ s^{-1}$, while the variants ranged from $16.7–31.8 \times 10^4\ M^{-1}\ s^{-1}$. In contrast, every clone dissociated slower than Vitaxin ($4.97 \times 10^{-3}\ s^{-1}$) with dissociation rates ranging from 1.6-fold ($3.03 \times 10^{-3}\ s^{-1}$) to 11.8-fold ($0.42 \times 10^{-3}\ s^{-1}$) slower.

Design of Combinatorial Library. It has been demonstrated that individual mutations can be combined to further enhance antibody affinity (29), enzyme activity (30), or protein stability (31). Random combination of all of the beneficial mutations of Vitaxin would generate a combinatorial library containing $>10^5$ variants, requiring efficient screening methodologies. Therefore, to determine whether clones displaying >10-fold enhanced affinities could be rapidly distinguished from one another, variants displaying 3- to 13-fold enhanced affinity were evaluated by capture lift using lower concentrations of biotinylated $\alpha_v\beta_3$. Despite repeated attempts with a broad range of concentrations of $\alpha_v\beta_3$, consistent differences in the capture lift signals were not observed. Because of this limitation, smaller combinatorial libraries were constructed and subsequently screened by ELISA.

Four distinct combinatorial libraries were constructed to evaluate the optimal number of combinations that could be accomplished by using hybridization mutagenesis. Uridinylated templates of Vitaxin and the three best light chain variants (Table 2; F32, N92, and L96) were prepared. Next, degenerate oligonucleotides encoding the wild-type residue and the most beneficial heavy chain mutations (Table 2; P60, H97, Y101, S102, T102, D102, E102, M102, G102, and A102) were hybridized to the light chain templates, resulting in four combinatorial libraries, each containing 64 unique variants. Potentially, the combination of multiple mutations may have detrimental effects on affinity, and thus may prevent the identification of beneficial combinations resulting from mutations at fewer sites. For this reason, the parental amino acid residue was included at each position in the combinatorial library. By using this approach, simultaneous combinatorial mutagenesis of three CDRs (L1 or L3 each in combination with H2 and H3) was accomplished.

Table 2. Identification of beneficial mutations from Vitaxin primary libraries

Chain	Library	Sequence	k_{on} ($\times 10^4$), $M^{-1}\ s^{-1}$	k_{off} ($\times 10^{-3}$), s^{-1}	K_d, nM
	Vitaxin		18.0	4.97	27.6
H	CDR1	G F T F S S Y D M S			
	T27	**T**	n.d.	n.d.	n.d.
	W29	**W**	n.d.	n.d.	n.d.
	L30	**L**	n.d.	n.d.	n.d.
H	CDR2a	W V A K V S S G G G			
	K52	**K**	17.8	2.18	12.2
H	CDR2b	S T Y Y L D T V Q G			
	P60	**P**	31.8	1.85	5.8
	E64	**E**	n.d.	n.d.	n.d.
H	CDR3	A R H N Y G S F A Y			
	H97	**H**	22.0	3.03	13.8
	Y100	**Y**	17.5	2.51	14.3
	D101	**D**	n.d.	n.d.	n.d.
	Y101	**Y**	21.8	0.48	2.2
	S102	**S**	24.2	1.44	6.0
	T102	**T**	24.6	1.43	5.8
	D102	**D**	27.6	0.97	3.5
	E102	**E**	n.d.	n.d.	n.d.
	M102	**M**	n.d.	n.d.	n.d.
	G102	**G**	16.1	2.01	12.5
	A102	**A**	27.5	2.27	8.3
L	CDR1	Q A S Q S I S N H L H W Y			
	F32	**F**	16.7	0.42	2.5
L	CDR2	L L I R Y R S Q S I S			
	S51	**S**	n.d.	n.d.	n.d.
L	CDR3	Q Q S G S W P H T			
	N92	**N**	23.6	1.35	5.7
	T92	**T**	n.d.	n.d.	n.d.
	L96	**L**	24.3	2.23	9.2
	Q96	**Q**	n.d.	n.d.	n.d.

n.d., not determined.

To screen the combinatorial libraries, soluble Fab was expressed and released from the periplasm of small-scale (<1 ml) bacterial cultures that had been infected with randomly selected clones. Although variable expression levels were observed, uniform quantities of the unpurified variants were captured on a microtiter plate through a peptide tag present on the carboxy-terminus of the heavy chain. As described (23), this assay enabled a rapid and direct comparison of the relative affinities of the variants after incubation with biotinylated $\alpha_v\beta_3$ and streptavidin-alkaline phosphatase. To ensure that the full Fab diversity was sampled, 1,000 randomly selected clones were screened from each combinatorial library. Variants that displayed an enhanced ELISA signal were further characterized for binding to immobilized $\alpha_v\beta_3$ (Fig. 1, ▲) and were sequenced to identify the mutations (Table 3).

Screening of the four combinatorial libraries identified 14 unique combinations of mutations that improved binding significantly over the individual mutations identified in the screening of the first library. Although the best clone from the primary screen had a 12.5-fold increase in affinity, the 14 unique combinations isolated from screening the combinatorial libraries displayed affinities ranging from 18- to 92-fold greater than Vitaxin. The majority of these variants consisted of H2 and H3 mutations combined with an L1 or L3 mutation. Beneficial combinations of heavy chain mutations with wild-type light chain also were identified, but did not result in improved affinity to the same extent as other combinatorial variants. The variants predominantly contained 2–4 mutations, with one clone, C29, containing five mutations. No direct correlation between the total number of mutations in each variant and the resulting affinity was observed. For example, whereas the binding of clone C37 was 92-fold enhanced over the parent molecule and was achieved through the combination of three mutations, clone C29 had ≈55-fold greater affinity achieved through the combination of five mutations. Multiple variants displaying >50-fold enhanced affinity resulting from the combination of as few as two mutations were identified (2G4, 17, and V357D).

The combinatorial clones with improved affinity all displayed >10-fold slower dissociation rates. In addition, all of the combinatorial variants isolated from the library based on the L96 light chain mutation also displayed 2- to 4-fold greater association rates. Previously it was demonstrated that the antibody repertoire shifts toward Igs displaying higher association rates during affinity maturation *in vivo* (32). The L96 subset of variants, therefore, may more closely mimic the *in vivo* affinity maturation process where B-lymphocyte proliferation is subject to a kinetic selection.

Characterization of Optimized Fabs. Vitaxin binds the $\alpha_v\beta_3$ complex specifically and does not recognize either the α_v or the β_3 chain separately. To further characterize the variants, clones were screened for reactivity with the related integrins, $\alpha_{IIb}\beta_3$ and $\alpha_v\beta_5$. All variants tested were unreactive with both $\alpha_{IIb}\beta_3$ and $\alpha_v\beta_5$, consistent with the improved binding not substantially altering the interaction of Fab and receptor (data not shown).

Table 3. Identification of optimal combinatorial mutations

Library	Clone	Sequence L1 32	L3 92	L3 96	H2 60	H3 97	H3 101	H3 102	k_{on} ($\times 10^4$), M^{-1} s^{-1}	k_{off} ($\times 10^{-3}$), s^{-1}	K_d, nM
Wild type		H	G	H	L	Y	A	Y	18.0	4.97	27.6
F32	17	**F**						**S**	25.1	0.138	0.5
	7	**F**			**P**	**H**		**S**	20.4	0.236	1.2
	56	**F**			**P**			**S**	26.6	0.135	0.5
	C59	**F**			**P**			**D**	26.5	0.137	0.5
	C176	**F**			**P**			**T**	22.5	0.192	0.9
	V357D	**F**						**D**	27.9	0.140	0.5
N92	C119		**N**		**P**			**S**	21.5	0.316	1.5
L96	8F9			**L**	**P**	**H**		**S**	47.5	0.280	0.6
	C29			**L**	**P**	**H**	**Y**	**S**	67.5	0.343	0.5
	2G4			**L**				**S**	60.3	0.229	0.4
	C37			**L**			**Y**	**E**	44.8	0.147	0.3
	6D1			**L**	**P**		**Y**	**S**	41.0	0.158	0.4
	6G1			**L**	**P**			**S**	38.9	0.280	0.7
	6H6			**L**		**H**		**S**	50.4	0.187	0.4

Next, we wanted to determine whether the increase in affinity of the variants resulted in greater biological activity. As a first step toward this, variants displaying a range of affinities were assayed for their ability to inhibit the binding of a natural ligand, fibrinogen, to immobilized $\alpha_v\beta_3$ receptor. As shown in Fig. 2*A* higher affinity variants were more effective at blocking the ligand binding site of the receptor (compare Vitaxin, ○, with any of the variants). Subsequent analysis of 10 variants displaying affinities (K_d) ranging from 0.3 to 27 nM demonstrated a good correlation ($r^2 = 0.976$) between affinity and ability to inhibit fibrinogen binding (Fig. 2*B*). In addition, the variants were tested for inhibition of vitronectin binding to the receptor. Similar to fibrinogen, the variants were more effective at inhibiting the interaction than the parent molecule (data not shown). Thus, consistent with the cross-reactivity studies with related integrin receptors, mutations that increased affinity did not appear to substantially alter the manner in which the antibody interacted with the receptor.

Finally, the ability of the variants to inhibit the adhesion of M21 human melanoma cells expressing the $\alpha_v\beta_3$ receptor to fibrinogen was examined. Similar to the ligand competition studies with purified fibrinogen and $\alpha_v\beta_3$ receptor, higher affinity variants were generally more effective at preventing cell adhesion than was Vitaxin (Fig. 3). Although intact Vitaxin IgG inhibits cell adhesion, the phage-expressed Fab did not affect cell adhesion at concentrations as high as 1 mg/ml (Fig. 3, ▲). Clone C37, isolated

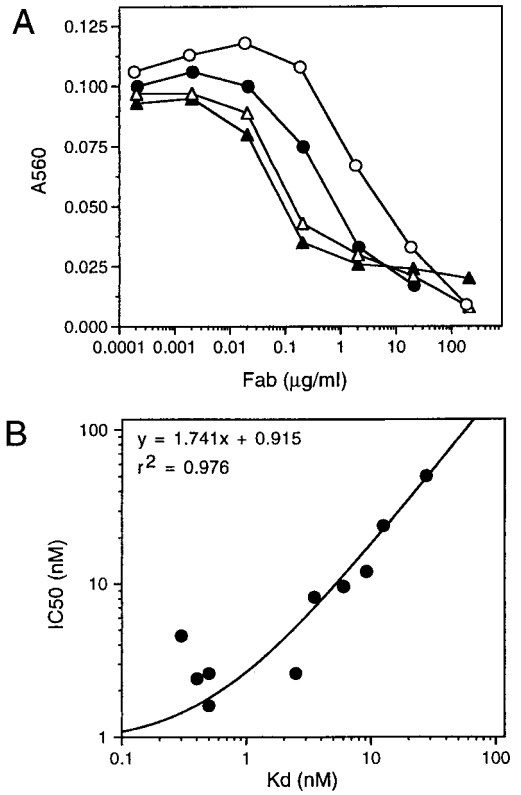

FIG. 2. (*A*) Inhibition of fibrinogen binding to immobilized $\alpha_v\beta_3$. Immobilized $\alpha_v\beta_3$ was incubated with 0.1 μg/ml of biotinylated fibrinogen and various concentrations of Vitaxin (○), S102 (●), F32 (△), or C59 (▲) for 3 h at 37°C. Unbound ligand and Fab were removed by washing, and bound fibrinogen was quantitated after incubation with NeutrAvidin alkaline phosphatase conjugate. (*B*) Correlation of affinity of variants with inhibition of fibrinogen binding. The concentration of variants required to inhibit the binding of fibrinogen to immobilized $\alpha_v\beta_3$ by 50% (IC_{50}) was plotted as a function of the affinity (K_d).

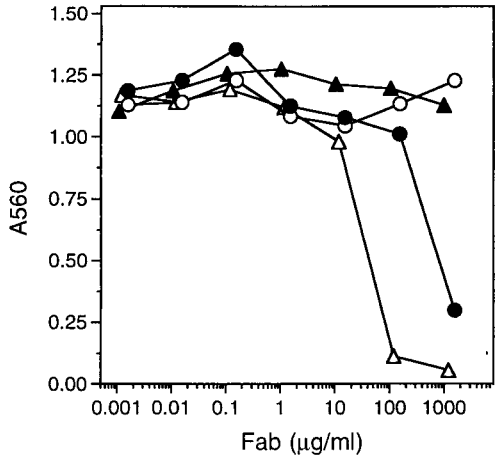

FIG. 3. Inhibition of M21 human melanoma cell adhesion to fibrinogen. Cells and various concentrations of Vitaxin Fab (▲), S102 (○), G102 (●), or C37 (△) were added to 96-well cell culture plates that had been coated with 10 μg/ml of fibrinogen. After incubating for 35 min at 37°C unbound cells were removed by washing, and adherent cells were quantitated by crystal violet staining.

from the combinatorial library and displaying ≈90-fold greater affinity than Vitaxin Fab, inhibited cell adhesion completely (Fig. 3, △). Variant G102 had a moderately higher affinity (2.2-fold enhanced) and also inhibited cell adhesion, though less effectively than C37 (Fig. 3, ●).

DISCUSSION

Evolution of proteins by natural selection is likely to occur through a series of steps consisting of small mutations that do not diminish function (33). One example of this process is the somatic hypermutation of antibody genes leading to affinity maturation *in vivo*. The stepwise nature of the process described in the present study was designed to mimic the evolution of proteins that occurs *in vivo*. Specifically, a random, limited, and iterative *in vitro* mutagenesis approach was used to optimize the affinity of Vitaxin >90-fold in the absence of structural information about the antigen or the antibody.

Initially, we reasoned that small incremental structural changes in the antibody were more likely to improve the affinity than large changes. Therefore, libraries consisting of Vitaxin variants with a single amino acid change at each CDR position were expressed and screened. The libraries created through this approach are considerably smaller than those constructed through total randomization. For example, for mutagenesis of an eight-residue CDR a library consisting of point mutations that introduces all 20 amino acids at every position would contain 160 unique clones. In contrast, complete randomization of the same CDR would yield $>10^{10}$ unique clones, of which only a minor fraction would be functional.

Several advantages were derived from using smaller libraries that introduce incremental structural changes. First, the lower complexity of the libraries resulted in the identification of variants with improved affinity with higher frequency than achievable in completely randomized libraries. Second, because the libraries were smaller and easily screened the contribution of all six CDRs to antigen binding was assessed. In contrast, random mutagenesis approaches typically either focus on a few specific residues or conversely, examine the entire variable region, including framework residues (reviewed in ref. 34). In the present study beneficial mutations were identified in all six CDRs. Finally, the small size of the libraries permitted the antibody variants to be screened in multiple formats, including plaque lift and ELISA. The engineering, therefore, was not affected by limitations typically associated with affinity enrichment, such as selection based on Fab display copy number or enrichment of clones with detrimental characteristics (undesired cross-reactivity, for example).

Rapid screening of small libraries (2,336 unique clones) containing point mutations led to the identification of multiple clones with 2- to 13-fold enhanced affinity. We assumed that some of these beneficial point mutations were at antibody sites that behave independently of one another. Construction, expression, and screening of a small combinatorial library (256 unique clones) verified this assumption. Multiple clones with 50- to 90-fold enhanced affinity, achieved through the combination of 2–5 mutations, were rapidly isolated after screening of the combinatorial library. Interestingly, one of the combinatorial variants, 2G4, displayed an affinity that was much greater than anticipated based on the affinities of the individual mutations before combining them. For example, 2G4 contains a mutation in L3 that alone enhances affinity 3-fold and, similarly, a mutation in H3 that enhances affinity ≈5-fold. The combined mutations, however, resulted in a variant with 69-fold higher affinity than the Vitaxin molecule. Thus, a sufficient percentage of the mutations behaved independently or semi-independently of one another to permit the rapid isolation of multiple improved variants after the screening of a library containing as few as 256 unique clones.

Finally, the variants were characterized to determine whether the functional properties of Vitaxin were retained. The specificity of the variants for the $\alpha_v\beta_3$ receptor complex was maintained as demonstrated by lack of cross-reactivity with the related integrins $\alpha_v\beta_5$ and $\alpha_{IIb}\beta_3$. In addition, similar to Vitaxin, the variants inhibited interaction of $\alpha_v\beta_3$ with both fibrinogen and vitronectin. In the case of fibrinogen, inhibition of receptor-ligand interaction was demonstrated by two approaches. In the first, coincubation of the variants with M21 cells overexpressing the $\alpha_v\beta_3$ receptor inhibited the adhesion of the cells to fibrinogen. In the second, the variants inhibited the binding of labeled fibrinogen to purified immobilized $\alpha_v\beta_3$ receptor. In the latter case, a direct correlation between affinity (K_d) and half-maximal inhibition of fibrinogen binding (IC_{50}) was observed, consistent with the variants maintaining the characteristics of Vitaxin.

Collectively, these studies describe the isolation of multiple Vitaxin variants with enhanced biological potency resulting from affinity maturation *in vitro*, which was accomplished while maintaining specificity for the $\alpha_v\beta_3$ complex. These improved versions may provide more potent versions of Vitaxin, possibly enhancing the therapeutic potential or permitting the administration of lower doses.

We gratefully acknowledge Lisa Manzuk for assisting in the *in vitro* characterization of variants and Dr. David A. Cheresh for helpful discussions.

1. Folkman, J. & Shing, Y. (1992) *J. Biol. Chem.* **267,** 10931–10934.
2. D'Amore, P. A. & Thompson, R. W. (1987) *Annu. Rev. Physiol.* **49,** 453–464.
3. Hanahan, D. & Folkman, J. (1996) *Cell* **86,** 353–364.
4. Folkman, J. (1995) *Nat. Med.* **1,** 27–31.
5. Friedlander, M., Theesfeld, C. L., Sugita, M., Fruttiger, M., Thomas, M. A., Chang, S. & Cheresh, D. A. (1996) *Proc. Natl. Acad. Sci. USA* **93,** 9764–9769.
6. Brooks, P. C., Clark, R. A. F. & Cheresh, D. A. (1994) *Science* **264,** 569–571.
7. Cheresh, D. A. (1987) *Proc. Natl. Acad. Sci. USA* **84,** 6471–6475.
8. Smith, J. W., Ruggeri, Z. M., Kunicki, T. J. & Cheresh, D. A. (1990) *J. Biol. Chem.* **265,** 12267–12271.
9. Enenstein, J., Waleh, N. S. & Kramer, R. H. (1992) *Exp. Cell Res.* **203,** 499–503.
10. Brooks, P. C., Clark, R. A. F. & Cheresh, D. A. (1994) *Science* **264,** 569–571.
11. Brooks, P. C., Montgomery, A. M. P., Rosenfeld, M., Reisfeld, R. A., Hu, T., Klier, G. & Cheresh, D. A. (1994) *Cell* **79,** 1157–1164.
12. Ausprunk, D. H., Knighton, D. R. & Folkman, J. (1975) *Am. J. Pathol.* **79,** 597–628.
13. Brooks, P. C., Stromblad, S., Klemke, R., Visscher, D., Sarkar, F. H. & Cheresh, D. A. (1995) *J. Clin. Invest.* **96,** 1815–1822.
14. Jones, P. T., Dera, P. H., Foote, J., Neuberger, M. S. & Winter, G. (1986) *Nature (London)* **321,** 522–525.
15. Rosok, M. J., Yelton, D. E., Harris, L. J., Bajorath, J., Hellström, K.-E., Hellström, I., Cruz, G. A., Kristensson, K., Lin, H., Huse, W. D. & Glaser, S. M. (1996) *J. Biol. Chem.* **271,** 22611–22618.
16. Kabat, E. A., Wu, T. T. & Bilofsky, H. (1977) *J. Biol. Chem.* **252,** 6609–6616.
17. Kabat, E. A., Wu, T. T., Perry, H. M., Gottesham, K. S. & Foeller, C. (1991) *Sequences of Proteins of Immunological Interest* (U. S. Department of Health and Human Services, Washington D.C.), 5th Ed.
18. Glaser, S. M., Yelton, D. E. & Huse, W. D. (1992) *J. Immunol.* **149,** 3903–3913.
19. Huse, W. D., Stinchcombe, T. J., Glaser, S. M., Starr, L., MacLean, M., Hellström, K. E., Hellström, I. & Yelton, D. E. (1992) *J. Immunol.* **149,** 3914–3920.
20. Kunkel, T. A. (1985) *Proc. Natl. Acad. Sci. USA* **82,** 488–492.
21. Smith, J. W. & Cheresh, D. A. (1988) *J. Biol. Chem.* **263,** 18726–18731.
22. Watkins, J. D., Beuerlein, G., Wu, H., McFadden, P. R., Pancook, J. D. & Huse, W. D. (1998) *Anal. Biochem.* **256,** 169–177.
23. Watkins, J. D., Beuerlein, G., Pecht, G., McFadden, P. R., Glaser, S. M. & Huse, W. D. (1997) *Anal. Biochem.* **253,** 37–45.
24. Field, J., Nikawa, J., Brock, D., MacDonald, B., Rodgers, L., Wilson, I. A., Lerner, R. A. & Wigler, M. (1988) *Mol. Cell. Biol.* **8,** 2159–2165.
25. Smith, J. W., Vestal, D. J., Irwin, S. V., Burke, T. A. & Cheresh, D. A. (1990) *J. Biol. Chem.* **265,** 11008–11013.
26. Leavesley, D. I., Ferguson, G. D., Wayner, E. A. & Cheresh, D. A. (1992) *J. Cell Biol.* **117,** 1101–1107.
27. Chothia, C. & Lesk, A. M. (1987) *J. Mol. Biol.* **196,** 901–917.
28. MacCallum, R. M., Martin, A. C. R. & Thornton, J. M. (1996) *J. Mol. Biol.* **262,** 732–745.
29. Yelton, D. E., Rosok, M. J., Cruz, G., Cosand, W. L., Bajorath, J., Hellström, I., Hellström, K. E., Huse, W. D. & Glaser, S. M. (1995) *J. Immunol.* **155,** 1994–2004.
30. Moore, J. C. & Arnold, F. H. (1996) *Nat. Biotechnol.* **14,** 458–467.
31. Sandberg, W. S. & Terwilliger, T. C. (1993) *Proc. Natl. Acad. Sci. USA* **90,** 8367–8371.
32. Foote, J. & Milstein, C. (1991) *Nature (London)* **352,** 530–532.
33. Macken, C. & Perelson, A. S. (1989) *Proc. Natl. Acad. Sci. USA* **86,** 6191–6195.
34. Marks, J. D., Hoogenboom, H. R., Griffiths, A. D. & Winter, G. (1992) *J. Biol. Chem.* **267,** 16007–16010.